

Recovery and reuse of floc sludge for high-performance capacitors

Di Zhang^{1,2}, Rong Hou¹, Wenbo Wang^{1,2}, He Zhao (✉)¹

¹ Beijing Engineering Research Center of Process Pollution Control, CAS Key Laboratory of Green Process and Engineering, Institute of Process Engineering, Chinese Academy of Sciences, Beijing 100190, China

² University of Chinese Academy of Sciences, Beijing 100049, China

HIGHLIGHTS

- The feasibility of facile fabrication of capacitor from floc sludge is discussed.
- The porous carbon composites are obtained by acidification and KOH activation.
- The as-prepared 3D structure has large surface area and optimal pore size.
- Admirable specific capacitance and outstanding cycling stability are obtained.

ARTICLE INFO

Article history:

Received 28 May 2021

Revised 14 September 2021

Accepted 14 September 2021

Available online 20 October 2021

Keywords:

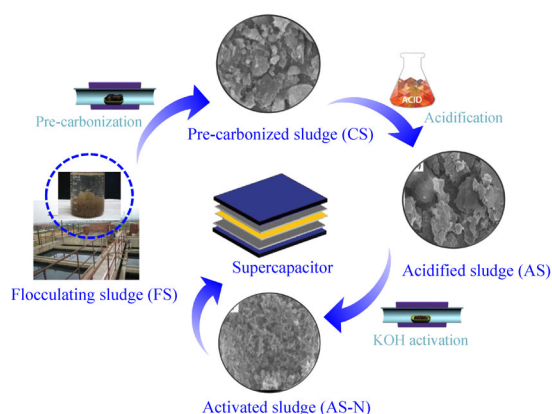
Floc sludge

Porous carbon electrode

Energy storage performance

Supercapacitors

GRAPHIC ABSTRACT



ABSTRACT

In this paper, floc sludge was transformed into porous carbon matrix composites by acidification and KOH activation at high temperature and used as an electrode material for application in capacitors. The effects of different treatment processes on the electrochemical properties of sludge materials were compared. The results of electrochemical tests showed that the sludge electrode exhibited excellent energy storage performance after HNO₃ acidification and KOH activation with a mass ratio of 3:1 (KOH/C). The specific capacitance of the sludge electrode reached 287 F/g at a current density of 1 A/g. In addition, the sludge electrode material showed excellent cycle stability (specific capacity retained at 93.4% after 5000 cycles at 5 A/g). Based on XRD, FTIR, SEM, TEM, and BET surface analysis, the morphology of sludge electrode materials can be effectively regulated by chemical pretreatment. The best-performing material showed a 3D porous morphology with a large specific surface area (2588 m²/g) and optimal pore size distribution, improving ion channels and charge conductivity. According to the life cycle assessment of floc sludge utilization, it reduced the resource consumption and toxicity risk by more than 90% compared with ordinary sludge disposal processes. This work provided a cost-effective and eco-friendly sludge reuse method and demonstrated the application potential of sludge-based materials in high-performance supercapacitors.

© Higher Education Press 2022

1 Introduction

With the acceleration of urbanization and industrial development, the treatment rate of urban sewage and industrial wastewater has increased year by year. In 2015,

there were more than 3000 sewage treatment plants in China, with an output of 40 million tons of sludge (moisture content of 80%), and 53% of sludge was not effectively and safely disposed (Li et al., 2018). Floc sludge is a kind of solid waste produced in the treatment of urban sewage and industrial wastewater. Sludge generated from industrial wastewater treatment often contains elevated concentrations of harmful contaminants, such as suspended solids, metal ions and organic pollutants, which

✉ Corresponding author

E-mail: hzhao@ipe.ac.cn

are detrimental to the environment and human health (Eid et al., 2019). Traditional sludge disposal methods such as land use (Laipan et al., 2017), landfills (Xiang et al., 2020), and incineration (Yui et al., 2018) are not sufficient to prevent secondary pollution caused by leaching, diffusion, and resuspension in the environment. Consequently, an effective stabilization and hazard-free treatment is highly needed. Sludge contains a large amount of carbon and metal salts. Currently, sludge derivatives such as “biosoil” (sludge and other material mixtures) (Giebułtowiec et al., 2020), energy (biogas (Feki et al., 2020; Wang et al., 2021), oil (Mirbagheri et al., 2015), heat (Jin et al., 2017), etc.), nutrients (phosphate (Wang et al., 2015b), nitrogen (Liu et al., 2019)) and metals (Mandal et al., 2011; Lin et al., 2021) are commonly implemented in practical applications. Sludge is also widely used as an adsorbent (Smith et al., 2009; Zhang et al., 2019) and water treatment carrier (Sadri Moghaddam et al., 2010) due to its similarity to clay.

Since most solid wastes are carbon-containing materials, much attention has been drawn to their excellent electrochemical properties. Wang et al. (Wang et al., 2008) formed a porous carbon material with excellent supercapacitance properties using Zn as a template to treat polytetrafluoroethylene solid waste. Ai et al. (Ai et al., 2017) prepared heteroatom-doped porous carbon extracted from tuna bones for high-performance lithium battery materials. Cao et al. (Cao et al., 2018) explored an electric Fenton cathode material from an anode material in a waste lithium battery for catalytic degradation. Wang et al. (Wang et al., 2013a) prepared carbon materials with adjustable pore diameters from pulp mill biological waste and applied them in the capacitor field. Wang et al. (Wang et al., 2015a) obtained a high-rate performance supercapacitor prepared from coal, and the capacitance of porous carbon reached 258 F/g at a current density of 1 A/g. At the same time, it has been noted that the electrochemical properties of carbon materials can be greatly improved by various types of pretreatment, including physical treatment with air, CO₂, seawater, and steam (Guo et al., 2020; Li et al., 2021) or chemical activation using acid (Li et al., 2012), KOH (Li et al., 2014; Feng et al., 2015), and ZnCl₂ (Wang et al., 2015a). The above studies have proven that a large amount of carbon-containing solid waste has good application potential in the electrochemical field for reuse.

The objective of this study was to prepare electrode materials from floc sludge by chemical activation. Different acidification treatments were adapted to improve the porous properties of oxygen-containing groups of carbonized sludge and remove impurities. Then, KOH activation was employed to further obtain a large specific surface area and a large number of microporous structures. The activated floc sludges were characterized to establish their textural properties and surface chemistry, and their

electrochemical characteristics were analyzed under different pretreatment processes. Based on these findings, a potential charge-storage mechanism was also proposed. In addition, the environmental impact of comprehensive sludge utilization was considered.

2 Materials and methods

2.1 Materials

Sludge was supplied by the coking wastewater treatment plant of Anshan Iron and Steel Co., Ltd. located in Anshan, Liaoning Province, China. All chemical reagents were of analytical grade and used as received without further purification. Ethanol, hydrofluoric acid, nitric acid, sulfuric acid, and potassium hydroxide (KOH) were purchased from Sinopharm Chemical Reagent Beijing Co., Ltd. (China). Polyvinylidene fluoride (PVDF), N,N-dimethylformamide (DMF) and acetylene black were purchased from Alfa Aesar (China) Chemical Co., Ltd.

2.2 Pretreatment of porous structured carbon derived from floc sludge

In a typical process, the raw floc sludge (FS) was dried and ground into a powder. Next, the FS powder was put in a tube furnace under nitrogen (N₂, 99.99%) flow. Then, 1 g of the obtained precarbonized sludge powder (CS) was impregnated in 2 mol/L HF, HNO₃, and H₂SO₄ solutions for acidification treatment for 8 h. The resulting acidified sludge samples were denoted AS-F, AS-N, and AS-S. After filtering and washing, equal quantities of KOH and 20 mL of pure water were added to the resulting powders, which were then stirred for 2 h and activated for 2 h from room temperature to 700°C under a nitrogen (N₂, 99.99%) atmosphere. The activated sludges were obtained and marked AS-F-1, AS-N-1, and AS-S-1. Furthermore, acidified sludge AS-N pretreated with HNO₃ was used to investigate the influence of different mass ratios of KOH on the structure and electrochemical performance of sludge materials. The resulting AS-N was then mixed with KOH at a KOH/C ratio of $x:1$ ($x = 1, 2, 3$ and 4) and activated by the method above. The samples activated by KOH with different KOH/C ratios of 1, 2, 3, and 4 were labeled AS-N-1, AS-N-2, AS-N-3, and AS-N-4, respectively (Fig.1). Under our experimental conditions, after carbonization and activation, the mass yield from the dry weight of raw floc sludge was 46%±8%. Based on the method reported by Tobiszewski et al. (2015), the mass intensity was calculated to be 1.74±0.28 kg/kg.

2.3 Preparation of the electrode material

The active material was obtained by mixing pretreated



Fig. 1 Schematic procedure for the fabrication of porous electrode material from floc sludge.

sludge, acetylene black and PVDF at a mass ratio of 8:1:1, followed by adding DMF at a mass ratio (active material: DMF) of 1:4. After the mixture was fully stirred for 12 h, the electrode slurry was prepared. Then, the prepared slurry was dropped evenly onto the surface of the 1 cm × 1 cm foamed nickel. The electrode material was thus obtained after drying at 60°C for 8 h.

2.4 Material characterization

X-ray diffraction (XRD) patterns were recorded with a PANalytical X-ray diffraction system (Empyrean, Netherlands) using Cu-K α ($\lambda = 1.5406$ nm) radiation. Fourier transform infrared spectroscopy (FTIR) analysis was performed by a T27 FT-IR spectrometer (Bruker, Switzerland). The morphology and microscopic structure of the activated sludge were characterized by using scanning electron microscopy (SEM, SU8020, Hitachi, Japan) and transmission electron microscopy (TEM, JEM-100CXII, JEOL, Japan). The specific surface area was evaluated by N₂ adsorption using a physisorption analyzer (Autosorb-iQ-MP, Quantachrome, USA).

2.5 Electrochemical measurements

The electrochemical characteristics of the pretreated sludge electrode were characterized by cyclic voltammetry (CV), galvanostatic charge/discharge (GCD) and electrochemical impedance spectroscopy (EIS) measurements in a conventional electrochemical cell. All electrochemical measurements were performed by an electrochemical workstation (Autolab PGSTAT 302N, Metrohm China Co. Ltd., Switzerland) in 6 M KOH at 25°C. The three-electrode system was applied in our study. A platinum slice (1 cm ×

1 cm) served as the auxiliary electrode. A Hg/HgO electrode (1 M NaOH) was prepared as the reference electrode.

The CV curves were recorded in the range of −1.0 to 0 V at a scan rate of 50 mV/s. The galvanostatic charge and discharge performance were measured at current densities ranging from 1 to 10 A/g. In our work, Eq. (1) was used to calculate the gravimetric specific capacitance, C_{GCD} (F/g): (Li et al., 2014; Rashidi and Yusup, 2020)

$$C_{\text{GCD}} = \frac{I \times \Delta t}{m \times \Delta U}, \quad (1)$$

where I is the charging and discharging current (A), Δt is the discharge duration (s), m is the active material quality (g), and ΔU is the variation in discharge voltage (V).

The Nyquist plots acquired from EIS analysis were acquired at an open circuit potential over a frequency range from 10⁴ to 0.01 Hz with an amplitude of 10 mV. All conducting wires, including the electrolytic cell, were shielded with a copper wire mesh to avoid electromagnetic interference. Evaluation and simulation (SIM) were employed by ZSimpWin software.

2.6 Environmental analysis

To estimate the environmental impact of floc sludge utilization, a life cycle assessment methodology was employed. The LCA according to ISO 14040 (2006) was used to perform this environmental analysis developed by using the LCA software eBalance (IKE, 2020). In this paper, the environmental impact of the sludge-based electrode material under different pretreatment conditions was compared with that of the traditional sludge incineration process. The functional unit was defined as 1 g of raw

floc sludge for carbon electrode material or disposal. The input data (chemicals, energy and water) were obtained from actual experimental data and the ecoinvent v3.1 database. All inventory data are provided in Table S1 in the supplementary materials.

3 Results and discussion

3.1 Morphological and structural characterization of raw and activated floc sludge

The morphology and microstructure of the resultant floc sludge activated by acidification and KOH were characterized by SEM and TEM. As shown in Figs. 2(a)–2(g), the sludge samples were all composed of uneven large particles with a diameter of 1–10 μm . Compared with the original sludge FS and precarbonized sludge CS, some cracks appeared on the surface of acidified sludge sample AS (Fig. 2(c)). Pore structure could be observed after continued activation by different amounts of KOH (Figs. 2(d)–2(g)). As the mass ratio of KOH/C increased to 3:1, the surface of sample AS-N-3 showed a clear porous structure, and the pore size was much smaller than that of AS-N-1 and AS-N-2. At the same time, an interconnected nanoscale porous network could also be observed with the accumulation of surface pores, indicating that there was a strong activation reaction between KOH and the sludge sample. However, the surface of the AS-N-4 sample was no longer porous, which may have resulted from certain collapse of the pore structure with excessive KOH activation (Yakaboylu et al., 2021).

The TEM images revealed the amorphous nature of

KOH-activated sludge, as shown in Figs. 2(h)–2(k). Heterogeneous mesopores with a size of 1–10 nm could also be observed. The morphological evolution of coagulated sludge after KOH activation was mainly due to the corrosion of carbon by KOH at high temperature. The carbon atoms in the sludge sample were aerified, and gases were released during the activation process (Fan et al., 2016; Li et al., 2020).

Figures 3(a) and 3(b) depict the FTIR results for floc sludge activated by acidification and KOH. The peaks located at 3449 cm^{-1} and 3437 cm^{-1} were ascribed to O-H vibrations. The peaks located at 2851 cm^{-1} , 2857 cm^{-1} , 2920 cm^{-1} , and 2930 cm^{-1} were ascribed to unsaturated C-H vibrations. The peak located at 1617 cm^{-1} was assigned to the C=C stretching vibration. The peak located at 1295 cm^{-1} was ascribed to the C=O absorption peak. The C1s XPS spectrum of FS (Fig. S1) also showed peaks corresponding to aromatics (C-C) (284.4 eV), aliphatics (C-C) (285.6 eV), and ketone groups (C=O) (287.6 eV). The peak located at 1085 cm^{-1} could be assigned to Si-O vibrations. Notable differences were found using different acidification methods. The Fe-O peak at 462 cm^{-1} disappeared in AS-F treated with HF, and the Si-O stretching vibration peak was also weakened. The C=O absorption peak intensity was higher in AS-N treated with HNO_3 than in the samples treated with the other two acids, indicating a higher degree of oxidation with more carboxyl functional groups in sludge, which helped to improve the mass transfer efficiency. Based on the peak located at 2073 cm^{-1} , the presence of C=C or cumulated double bonds could be confirmed. The results demonstrated that the content of unsaturated carbon (i.e., oxygen-containing functional groups) increased after KOH activation at high

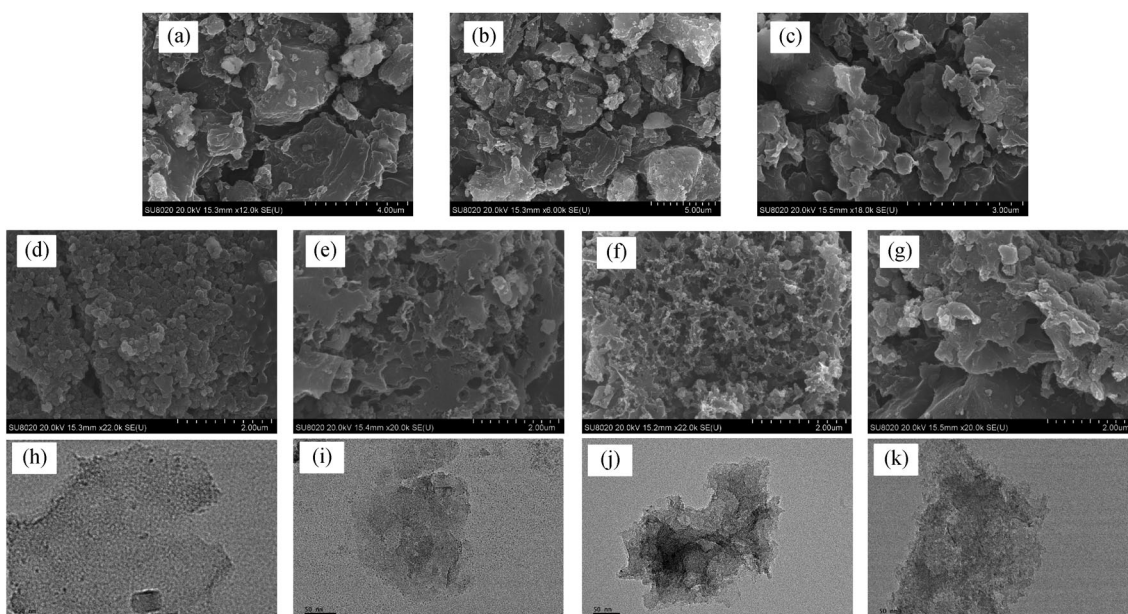


Fig. 2 SEM (a–g) and TEM (h–k) images of floc sludges: FS (a), CS (b), AS (c), AS-N-1 (d, h), AS-N-2 (e, i), AS-N-3 (f, j), and AS-N-4 (g, k).

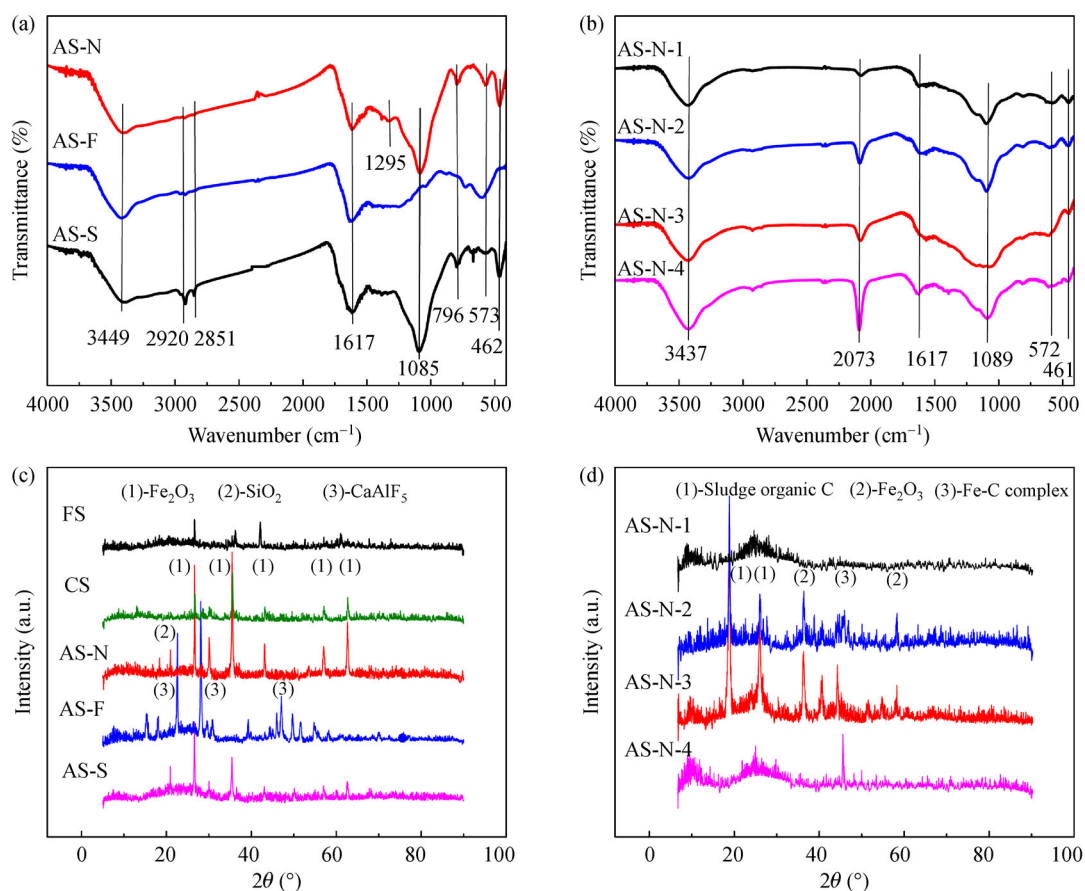


Fig. 3 FTIR spectra and XRD patterns of floc sludge pretreated with different acids (a, c) and treated with different mass ratios of KOH (b, d).

temperatures, which was consistent with previous reports (Muniandy et al., 2014; Liang et al., 2020).

Figures 3(c) and 3(d) show the XRD patterns of precarbonized, acidified and KOH-activated samples in the 2-theta range of 5°–90°. As shown in Fig. 3(c), with the precarbonization and acidification treatment, the original sludge (FS) was transformed to a crystalline structure from an amorphous state: the crystallinity of the sludge increased gradually, and the molecular arrangement in the material tended to be an ordered structure. In addition, the characteristic diffraction peaks of iron oxide and silicon dioxide in the AS-F sample disappeared. Instead, the fluoride peak appeared. The crystallinity of the AS-N sample was slightly better than that of AS-F, and AS-S could also be observed. It could be inferred that the AS-N sample had better electrochemical performance due to its multifunctional group characteristics and high crystallinity. Moreover, according to Fig. 3(d), with the addition of KOH, the crystallinity first increased and then decreased. Sample AS-N-3 had the highest crystallinity and was relatively orderly when the mass ratio of KOH/C was 3:1, which is consistent with the SEM and TEM results.

The N₂ adsorption-desorption isotherms and pore size distribution obtained for the resulting samples of AS-N-1,

AS-N-2, AS-N-3 and AS-N-4 are displayed in Fig. 4, and the details are demonstrated in Table 1, which could indicate the influence of different KOH ratios on the pore structure of floc sludge material. The specific surface area (S_{BET}) was calculated by the BET method reported previously (Xia et al., 2013). As shown in Fig. 4(a), the specific surface area, as well as the total pore volume, could be amplified with increasing KOH amount. Therefore, the AS-N-3 sample had the largest BET specific surface area, and the AS-N-4 sample had the highest total pore volume. The S_{BET} and V_{total} of AS-N-3 even reached 2588 m²/g and 1.82 cm³/g, respectively. These two parameters were much higher than those of AS-N-1 (S_{BET} : 1279 m²/g; V_{total} : 1.38 cm³/g). All the samples showed hysteresis loops when the relative pressure (P/P_0) was 0.9–1.0, indicating the existence of mesoporous structures. At the same time, the sludge samples contained several mesoporous and macroporous structures, which were due to surface accumulation.

Figure 4(b) shows the pore volume and pore size distribution of the sludge samples, which were obtained by nonlocal density function theory (NLDFT). A large number of micropores were identified with pore sizes concentrated between 0.5 and 6 nm. The curves showed a

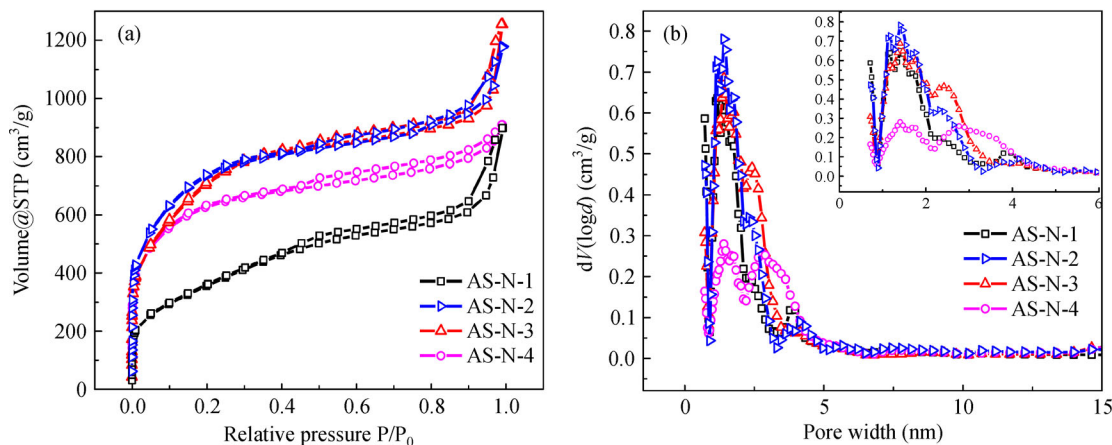


Fig. 4 N₂ adsorption–desorption isotherms (a) and pore size distribution (b) of sludge samples treated with different mass ratios of KOH/C (pressure of 10⁻⁵ Pa to ambient pressure at a nitrogen boiling point of 77K).

Table 1 Surface area and textural properties of sludge treated with different mass ratios of KOH

Samples	$S_{\text{BET}}^{1)}$ (m ² /g)	$V_{\text{micro}}^{2)}$ (cm ³ /g)	$V_{\text{total}}^{3)}$ (cm ³ /g)	$V_{\text{micro}}/V_{\text{total}}$ (%)
AS-N-1	1279	0.54	1.38	39.13
AS-N-2	2241	0.61	1.51	40.39
AS-N-3	2588	0.81	1.82	44.51
AS-N-4	2480	0.67	1.94	34.53

Notes: 1) S_{BET} : specific surface area, 2) V_{micro} : micropore volume, 3) V_{total} : total pore volume.

multi-peak pore diameter distribution, which indicated the multiscale pore sizes in the porous structure. Multiscale pore size structures were beneficial to improve the electrochemical performance of the supercapacitor device. The mesopores provided low-resistance channels for the ions, while the microporous channels provided a place for effective charge accumulation (Yue et al., 2019). The micropore volume of AS-N-3 accounted for the largest proportion (44.51%) of the total micropore volume, which facilitated ion transport through the electrolyte and improved its capacity for electrochemical energy storage. However, when the KOH/C ratio further increased to 4:1, the decline in the number of microporous structures and the collapse of pore structures resulted in a decrease in the surface area of the sludge material.

In terms of elemental analysis (Table S2), pyrolysis of the floc sludge decreased the oxygen content, which consequently resulted in an increased fixed carbon and iron content. In addition, potassium and nitrogen also showed increased levels, which might be due to the addition of HNO₃ and KOH. The changes in the elemental proportions showed that higher carbon and iron contents were beneficial to electron transportation after carbonization.

In contrast to other papers, floc sludge containing natural

Fe is used as a raw material in this paper to increase the conductivity of carbon materials. During the carbonization of acid-based sludge, the formation of nitrate/sulfate/fluoride species occurs, and these species are chemically bound inside the pore structure of sludge-derived carbons. It could help to improve the mass transfer efficiency with more carboxyl functional groups attached. The KOH activation method adopted in this paper could further enhance the existing pores and create new pores. Based on the synergistic effect of the above three factors, carbonized sludge produced better properties for electrochemical applications.

3.2 Electrochemical performance of the sludge electrode

Figure 5 reveals the electrochemical characterization of sludge materials after different acidification processes and KOH activation with a mass ratio of 1:1. According to the CV curves (Fig. 5(a)), the profiles of the sludge electrode materials exhibited a quasi-rectangular CV curve without noticeable redox peaks at the same scanning speed, indicating good double-layer capacitive behaviors. The integral area of the CV curves of the AS-N-1 material was larger than that of the others, which indicated the largest electrochemical capacitance. All three samples exhibited triangle-like charge/discharge curves at a current density of 1 A/g (Fig. 5(b)), manifesting reversible capacitive behaviors.

To account for the electrochemical performance of different sludge electrode materials, EIS was performed with three different cathodes (shown in Fig. 5(c)). In general, the semicircle diameter of the high-frequency region represents the charge-transfer resistance, R_{ct} , at the electrode surface. The diameters of the semicircular region were 22 Ω , 24 Ω , and 37 Ω for AS-N-1, AS-F-1, and AS-S-1, respectively, indicating lower charge-transfer resistance in AS-N-1. According to the analysis of the structural

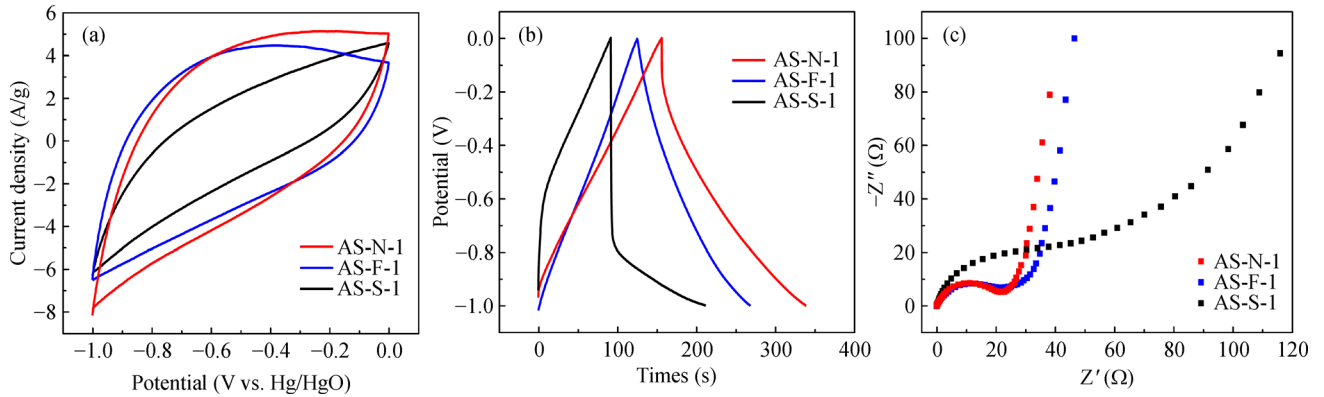


Fig. 5 (a) CV curves, (b) GCD curves, and (c) Nyquist curves of AS-N-1, AS-F-1, and AS-S-1. (mass ratio of the sludge material to KOH = 1:1, scan rate = 50 mV/s, voltage range = $-0.1-0$ V, and current density = 1 A/g).

characteristics above, carboxylic and other functional groups on the surface of AS-N-1 might speed up electronic mass transfer and thus reduce the internal resistance of the sludge material.

Figure 6 reveals the electrochemical characterization of sludge materials treated by the HNO_3 acidification process followed by KOH activation with a mass ratio of 1:1–4:1. The CV curves of AS-N-1, AS-N-2, AS-N-3 and AS-N-4 are shown Fig. 6(a). All the profiles of the electrode materials exhibited a quasi-rectangular-shaped CV curve without noticeable redox peaks at a scan rate of 50 mV/s, which showed good double-layer capacitive behaviors. The integral area of the CV curves of AS-N-3 was the largest among the four samples, indicating the largest electrochemical capacitance of AS-N-3. As shown in Fig. 6(b), there was a gradual decrease in the current response and a slight deviation from the ideal rectangular shape as the scan rate decreased in the CV curve of the AS-N-3 electrode, indicating that the electrolyte ions exhibited a rapid ionic response at a scan rate of 50 mV/s. To further investigate the differences in the structure and electrochemical performance of the different KOH-activated samples, EIS analysis was performed. According to

Fig. 6(c), AS-N-3 had the smallest semicircular diameter in the high-frequency region and the straightest line in the low-frequency region, indicating the lowest charge-transfer resistance.

Based on the above analysis, it can be concluded that it is more beneficial for electrolyte ion diffusion and charge transfer with additional KOH in sludge samples, which was also supported by the specific surface area, as well as the micropore volume results in Fig. 4 and Table 1.

Considering the excellent porous properties and electrochemical characteristics, it is reasonable to expect that the treated sludge materials will have certain application value in the supercapacitor field. Therefore, the energy storage performance of the sludge electrodes was investigated by testing the GCD curves at a current density of 1 A/g. As seen in Fig. 7(a), the GCD curves of AS-N-1 and AS-F-1 exhibited isosceles triangle-like shapes, while AS-S-1 was slightly deviated from the ideal triangular shape. The highest specific capacitance value calculated from the GCD curves was found in AS-N-1 (210 F/g). The results confirmed that the ideal capacitive behaviors of the AS-N-1 electrode material and the energy storage mechanism were mainly due to double-layer energy storage, which

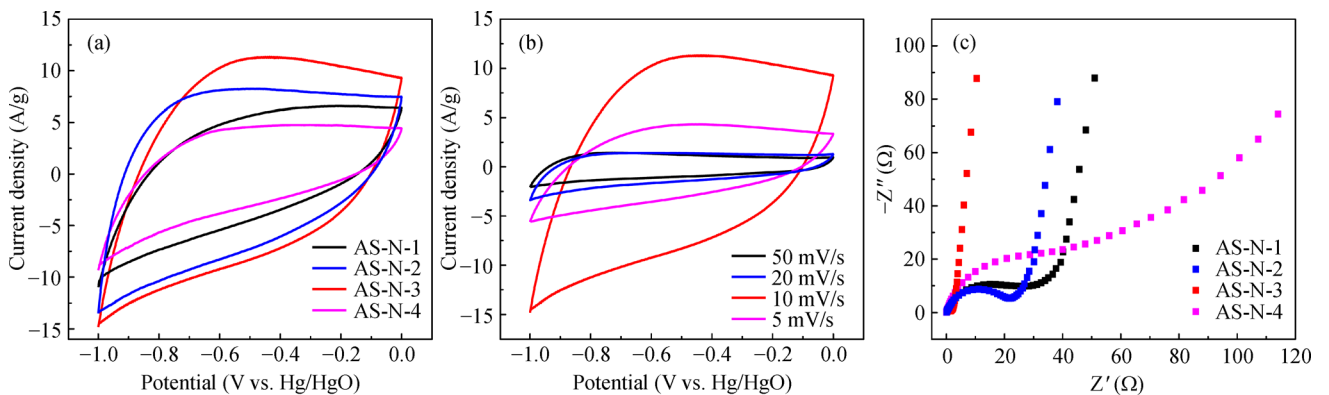


Fig. 6 (a) CV curves of AS-N-1, AS-N-2, AS-N-3, and AS-N-4. (b) CV curves of AS-N-3 at different scan rates. (c) Nyquist curves of AS-N-1, AS-N-2, AS-N-3, and AS-N-4. (Scan rate = 50 mV/s and voltage range = $-0.1-0$ V).

was consistent with the cyclic voltammetry study (Fig. 5 (a)).

Figure 7(b) reveals the GCD curves of sludge materials treated by the HNO_3 acidification process followed by activation with different amounts of KOH. The results showed that all the samples exhibited isosceles triangle-like shapes, which confirmed the ideal electronic double layer capacitor (EDLC) of the materials activated by KOH. The AS-N-3 sample achieved the highest specific capacitance of 287 F/g at 1 A/g, which verified good energy storage properties. The specific capacitance in our study was similar to or higher than that of other reported capacitors made by the utilization of carbon materials (Mitravinda et al., 2018; Xu et al., 2020; Yakaboylu et al., 2021). The high specific capacitance and energy density could be explained by the presence of more micropores and the large surface area of the AS-N-3 material.

Isosceles triangle-like shapes could also be observed at different charge–discharge current densities in the AS-N-3 material (Fig. 7(c)), further indicating its nearly ideal capacitive performance. As shown in Fig. 7(d), the specific capacitance of AS-N-3 decreased as the current density increased, which could be explained by the ion diffusion

mechanism. Owing to the amorphous porous structure of floc sludge materials after carbonization and pretreatment processes, the interface diffusion resistance of the electrolyte in the electrode was increased at high current densities. When the current density reached 10 A/g, the specific capacitance of AS-N-3 could still be kept at 66.8%, showing excellent rate performance and great potential for energy storage applications.

As the excellent supercapacitance performance of AS-N-3 is shown in Fig. 7, it is now necessary to analyze the stability of the sludge electrode material. The long-term stability of AS-N-3 is demonstrated by the specific capacitance as a relationship curve of cycle numbers at 5 A/g (Fig. 8). After 500 cycles, the specific capacity was retained at ~ 211 F/g, corresponding to $\sim 99.6\%$ of its original value. A main reason for the capacitance loss of sludge-based supercapacitors was the dissolution of active materials into electrolyte solution during cycling (Wang et al., 2013b). Afterward, in our experiment, the capacitance was 93.4% of the initial capacitance after 5000 charge-discharge cycles, indicating the excellent long-term stability of the electrode. The durability of the sludge-based material in cycling was generally consistent with the

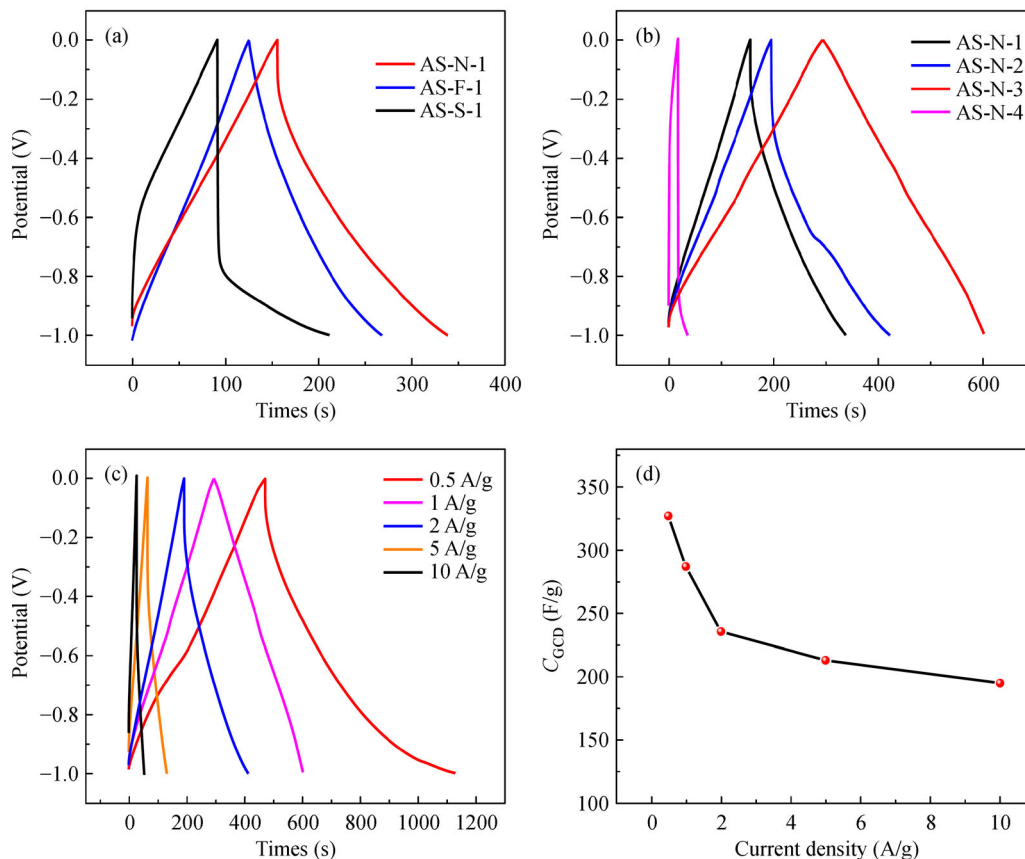


Fig. 7 Galvanostatic charge-discharge curves and specific capacitance of pretreated sludge materials: (a) AS-N-1, AS-F-1, and AS-S-1 from sludge pretreated with different acids and (b) AS-N-1, AS-N-2, AS-N-3 and AS-N-4 from sludge treated with different mass ratios of KOH ((a, b) current density = 1 A/g). (c) Galvanostatic charge-discharge curve of AS-N-3 (current density were measured at 0.5, 1, 2, 5, and 10 A/g). (d) Specific capacitance of AS-N-3 (current density were measured at 0.5, 1, 2, 5, and 10 A/g).

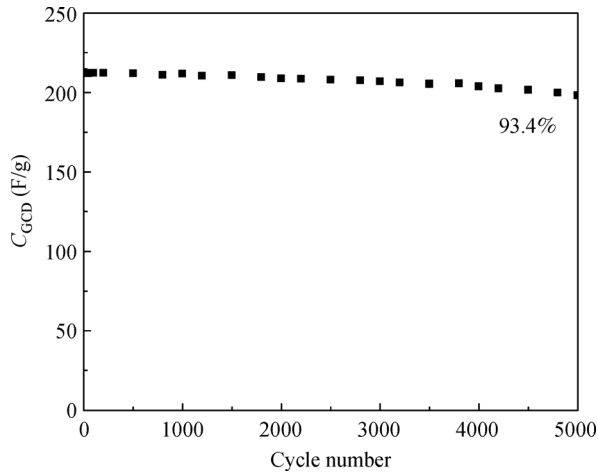


Fig. 8 Cycling stability of AS-N-3 at a current density of 5 A/g.

results reported in the literature, which are in the range of 5%–10% losses in 5000 cycles (Li et al., 2017; Lei et al.,

2020). Thus, all the results indicated that the sludge-based material is promising for practical industrial applications in supercapacitors.

3.3 Life cycle assessment of sludge electrode materials

To further verify the practical feasibility, a comprehensive assessment was adapted in this paper by evaluating the environmental impact of sludge recovery and utilization. The normalized environmental impacts of the six carbon electrode preparation processes are exhibited in Fig. 9. In traditional processes, sludge disposal primarily leads to toxicity risks and climate change influences. Therefore, carbon emissions (CEs), the Chinese fossil fuel depletion potential (CADP), the ecological ecotoxicity potential (ET) and the human toxicity potential (HT) were chosen as the main assessment indices.

Figure 9(a) shows the normalized emission contribution for CO₂. Sludge-based electrode sample AS-F-1 occupied the largest carbon footprint. Wherein, the carbon footprints

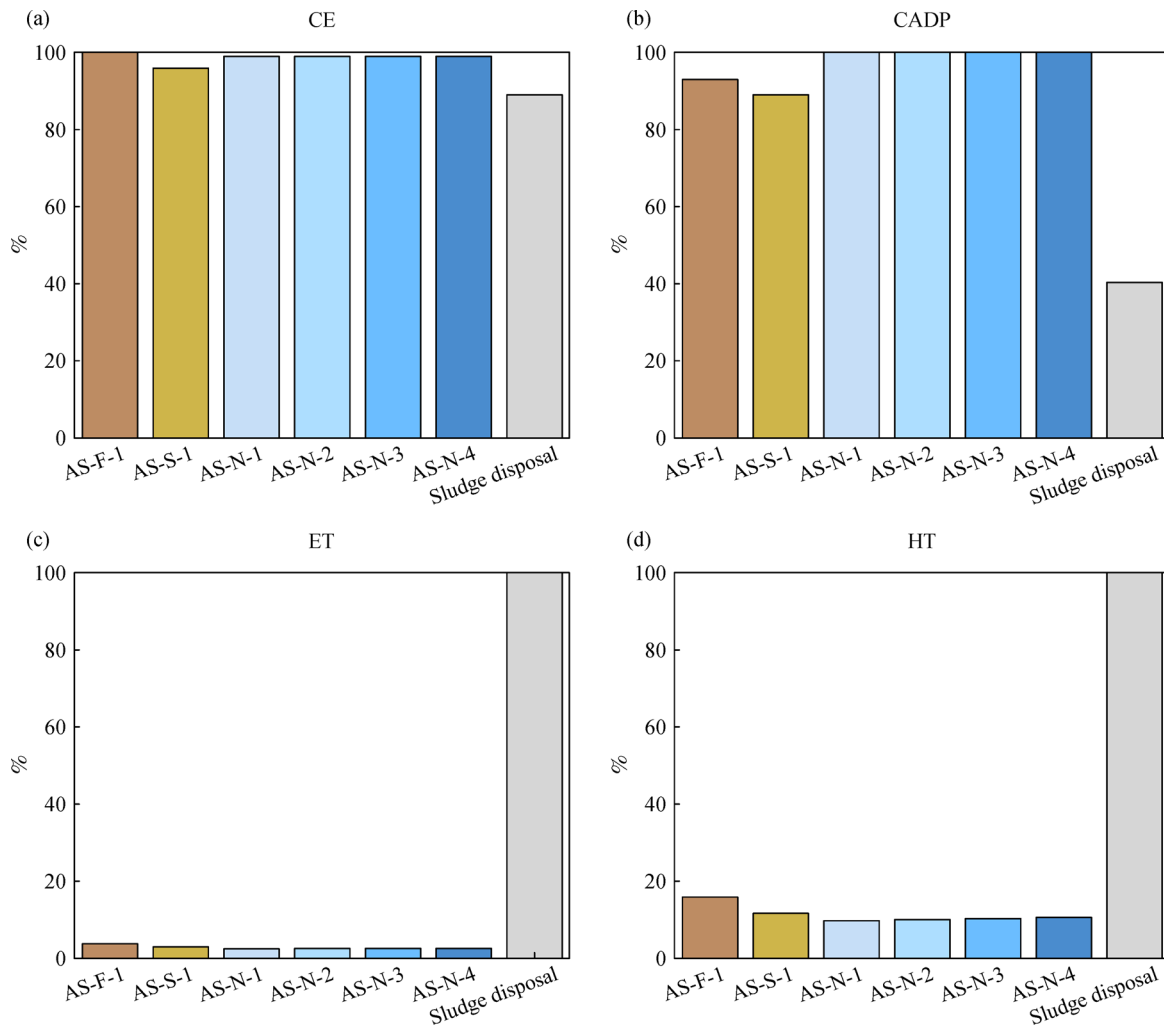


Fig. 9 Percentage contribution of environmental impact categories to 1 g dried sludge material powder utilization. (a) Carbon emissions (CEs), (b) Chinese fossil fuel depletion potential (CADP), (c) ecological ecotoxicity potential (ET), and (d) human toxicity potential (HT).

of AS-N samples were 1% lower. For the sludge disposal process, the contribution was 11% lower than that of AS-F-1. The main source of CO₂ emissions from traditional sludge disposal was the combustion of organic matter in sludge (Liu et al., 2020). However, the use of electricity (>70% contribution) and different acids (>20% contribution) in electrode preparation processes increased carbon emissions to a certain degree.

As seen in Fig. 9(b), the CADP of sludge disposal was maximal, with a decrease of 91% in the six electrode material preparation process. In the sludge disposal process, the large amounts of electricity and polyacrylamide used were responsible for over 70% of resource consumption. Compared with the traditional sludge combustion method, this paper recycled sludge to make carbon electrodes, which reduced electricity consumption and other energy-consuming raw materials. In practical applications, it saved the amount of fossil fuel and resources consumed. In terms of ET (Fig. 9(c)) and HT (Fig. 9(d)), the sludge disposal results were far higher than those of the six electrode preparation processes. The ET and HT in electrode preparation processes accounted for 3%–4% and 10%–16% in the sludge disposal process, respectively. The direct reason for the results was the large amount of chemicals used and toxic substances released from sludge incineration, such as SO₂, CO, NO, HF, and dioxin. The recycling of sludge materials in this paper could reduce the impact on the ecological environment and human body.

Therefore, although few strong acids were used in this paper, leading to an 11% increase in carbon emissions, they reduced resource consumption and the toxicity risk by more than 90% compared with ordinary sludge disposal processes.

4 Conclusions

In summary, we developed a facile resource utilization method by reusing floc sludge for carbon matrix electrodes with porous channels and high conductivity. The chemical activation reaction was of great importance to porous structure formation and evolution. The as-prepared sample AS-N-3 had a 3D porous structure with a large specific surface area (2588 m²/g) and an optimal pore size distribution. In addition to simple fabrication, the electrodes prepared by this method exhibited excellent electrochemical performance. The rational porous structure of AS-N-3 resulted in an admirable specific capacitance (287 F/g at 1 A/g), good rate capacity (66.8% retention at 10 A/g), and outstanding cycling stability (93.4% retention after 5000 cycles in a supercapacitor). The recycling of sludge materials in this paper could reduce the impact on the ecological environment and human body by more than 90%. This work not only provides a cost-effective strategy

to synthesize hierarchical porous carbon as an electrode material for high-performance supercapacitors but also offers a promising method for the large-scale fabrication of energy storage materials from hazardous industrial waste.

Acknowledgements We gratefully acknowledge the funding by National Natural Science Foundation of China (Grant No. 51978643) and Youth Innovation Promotion Association, CAS (2014037).

Electronic Supplementary Material Supplementary material is available in the online version of this article at <https://doi.org/10.1007/s11783-021-1512-5> and is accessible for authorized users.

References

- Ai F, Liu N, Wang W, Wang A, Wang F, Zhang H, Huang Y (2017). Heteroatoms-doped porous carbon derived from tuna bone for high performance Li-S batteries. *Electrochimica Acta*, 258: 80–89
- Cao Z, Zheng X, Cao H, Zhao H, Sun Z, Guo Z, Wang K, Zhou B (2018). Efficient reuse of anode scrap from lithium-ion batteries as cathode for pollutant degradation in electro-Fenton process: Role of different recovery processes. *Chemical Engineering Journal*, 337: 256–264
- Eid E M, Alrumman S A, Galal T M, El-Bebany A F (2019). Regression models for monitoring trace metal accumulations by *Faba sativa* Bernh. plants grown in soils amended with different rates of sewage sludge. *Scientific Reports*, 9(1): 5443
- Fan L, Liu P F, Yan X, Gu L, Yang Z Z, Yang H G, Qiu S, Yao X (2016). Atomically isolated nickel species anchored on graphitized carbon for efficient hydrogen evolution electrocatalysis. *Nature Communications*, 7(1): 10667
- Feki E, Battimelli A, Sayadi S, Dhoubi A, Khoufi S (2020). High-rate anaerobic digestion of waste activated sludge by integration of electro-Fenton process. *Molecules (Basel, Switzerland)*, 25(3): 626
- Feng H, Zheng M, Dong H, Xiao Y, Hu H, Sun Z, Long C, Cai Y, Zhao X, Zhang H, Lei B, Liu Y (2015). Three-dimensional honeycomb-like hierarchically structured carbon for high-performance supercapacitors derived from high-ash-content sewage sludge. *Journal of Materials Chemistry. A, Materials for Energy and Sustainability*, 3(29): 15225–15234
- Giebułtowicz J, Nałęcz-Jawecki G, Hamisz M, Kucharski D, Korzeniewska E, Płaza G (2020). Environmental risk and risk of resistance selection due to antimicrobials' occurrence in two polish wastewater treatment plants and receiving surface water. *Molecules (Basel, Switzerland)*, 25(6): 1470
- Guo M, Song W, Tian J (2020). Biochar-facilitated soil remediation: mechanisms and efficacy variations. *Frontiers in Environmental Science*, 8: 521512
- IKE (2020). eBalance v.4.7.14122.518. Chengdu: IT Knowledge & Education
- Jin Z, Ji F, He Y, Zhao M, Xu X, Zheng X Y (2017). Evaluating the efficiency of carbon utilisation via bioenergetics between biological aerobic and denitrifying phosphorus removal systems. *PLoS One*, 12(10): e0187007
- Laipan M, Fu H, Zhu R, Sun L, Zhu J, He H (2017). Converting spent

- Cu/Fe layered double hydroxide into Cr(VI) reductant and porous carbon material. *Scientific Reports*, 7(1): 7277
- Lei Z, Liu L, Zhao H, Liang F, Chang S, Li L, Zhang Y, Lin Z, Kröger J, Lei Y (2020). Nanoelectrode design from microminiaturized honeycomb monolith with ultrathin and stiff nanoscaffold for high-energy micro-supercapacitors. *Nature Communications*, 11(1): 299
- Li M, Liu C, Cao H, Zhao H, Zhang Y, Fan Z (2014). KOH self-templating synthesis of three-dimensional hierarchical porous carbon materials for high performance supercapacitors. *Journal of Materials Chemistry. A, Materials for Energy and Sustainability*, 2(36): 14844–14851
- Li T, Ma R, Lin J, Hu Y, Zhang P, Sun S, Fang L (2020). The synthesis and performance analysis of various biomass - based carbon materials for electric double-layer capacitors: A review. *International Journal of Energy Research*, 44(4): 2426–2454
- Li X, Chen L, Mei Q, Dong B, Dai X, Ding G, Zeng E Y (2018). Microplastics in sewage sludge from the wastewater treatment plants in China. *Water Research*, 142: 75–85
- Li X, Hao T, Tang Y, Chen G (2021). A “Seawater-in-Sludge” approach for capacitive biochar production via the alkaline and alkaline earth metals activation. *Frontiers of Environmental Science & Engineering*, 15(1): 3
- Li X, Liu K, Liu Z, Wang Z, Li B, Zhang D (2017). Hierarchical porous carbon from hazardous waste oily sludge for all-solid-state flexible supercapacitor. *Electrochimica Acta*, 240: 43–52
- Li Z, Zhang L, Amirkhiz B S, Tan X, Xu Z, Wang H, Olsen B C, Holt C M B, Mitlin D (2012). Carbonized chicken eggshell membranes with 3D architectures as high-performance electrode materials for supercapacitors. *Advanced Energy Materials*, 2(4): 431–437
- Liang Q, Liu Y, Chen M, Ma L, Yang B, Li L, Liu Q (2020). Optimized preparation of activated carbon from coconut shell and municipal sludge. *Materials Chemistry and Physics*, 241: 122327
- Lin X, Chen X, Li S, Chen Y, Wei Z, Wu Q (2021). Sewage sludge ditch for recovering heavy metals can improve crop yield and soil environmental quality. *Frontiers of Environmental Science & Engineering*, 15(2): 22
- Liu W, Iordan C M, Cherubini F, Hu X, Fu D (2020). Environmental impacts assessment of wastewater treatment and sludge disposal systems under two sewage discharge standards: A case study in Kunshan, China. *Journal of Cleaner Production*, 287: 125046
- Liu X, Liu L, Leng P, Hu Z (2019). Feasible and effective reuse of municipal sludge for vegetation restoration: physiochemical characteristics and microbial diversity. *Scientific Reports*, 9(1): 879
- Mandal B K, Vankayala R, Uday Kumar L (2011). Speciation of chromium in soil and sludge in the surrounding tannery region, ranipet, Tamil Nadu. *ISRN Toxicology*, 2011: 697980
- Mirbagheri M, Nahvi I, Emamzade R (2015). Reduction of chemical and biological oxygen demands from oil wastes via oleaginous fungi: an attempt to convert food by products to essential fatty acids. *Iranian Journal of Biotechnology*, 13(2): 25–30
- Mitrovinda T, Nanaji K, Anandan S, Jyothirmayi A, Chakravadhanula V S K, Sharma C S, Rao T N (2018). Facile synthesis of corn silk derived nanoporous carbon for an improved supercapacitor performance. *Journal of the Electrochemical Society*, 165(14): A3369–A3379
- Muniandy L, Adam F, Mohamed A R, Ng E P (2014). The synthesis and characterization of high purity mixed microporous/mesoporous activated carbon from rice husk using chemical activation with NaOH and KOH. *Microporous and Mesoporous Materials*, 197: 316–323
- Rashidi N A, Yusup S (2020). Recent methodological trends in nitrogen-functionalized activated carbon production towards the gravimetric capacitance: A mini review. *Journal of Energy Storage*, 32: 101757
- Sadri Moghaddam S, Alavi Moghaddam M R, Arami M (2010). Coagulation/flocculation process for dye removal using sludge from water treatment plant: optimization through response surface methodology. *Journal of Hazardous Materials*, 175(1–3): 651–657
- Smith K M, Fowler G D, Pullket S, Graham N J (2009). Sewage sludge-based adsorbents: a review of their production, properties and use in water treatment applications. *Water Research*, 43(10): 2569–2594
- Tobiszewski M, Marć M, Gałuszka A, Namieśnik J (2015). Green chemistry metrics with special reference to green analytical chemistry. *Molecules (Basel, Switzerland)*, 20(6): 10928–10946
- Wang D W, Li F, Liu M, Lu G Q, Cheng H M (2008). 3D aperiodic hierarchical porous graphitic carbon material for high-rate electrochemical capacitive energy storage. *Angewandte Chemie (International ed. in English)*, 120(2): 379–382
- Wang H, Li Z, Tak J K, Holt C M B, Tan X, Xu Z, Amirkhiz B S, Harfield D, Anyia A, Stephenson T, Mitlin D (2013a). Supercapacitors based on carbons with tuned porosity derived from paper pulp mill sludge biowaste. *Carbon*, 57: 317–328
- Wang L, Wang R, Zhao H, Liu L, Jia D (2015a). High rate performance porous carbon prepared from coal for supercapacitors. *Materials Letters*, 149: 85–88
- Wang L, Yang C, Thangavel S, Guo Z, Chen C, Wang A, Liu W (2021). Enhanced hydrogen production in microbial electrolysis through strategies of carbon recovery from alkaline/thermal treated sludge. *Frontiers of Environmental Science & Engineering*, 15(4): 56
- Wang T, Peng Z, Wang Y, Tang J, Zheng G (2013b). MnO nanoparticle@mesoporous carbon composites grown on conducting substrates featuring high-performance lithium-ion battery, supercapacitor and sensor. *Scientific Reports*, 3(1): 2693
- Wang Y K, Pan X R, Geng Y K, Sheng G P (2015b). Simultaneous effective carbon and nitrogen removals and phosphorus recovery in an intermittently aerated membrane bioreactor integrated system. *Scientific Reports*, 5(1): 16281
- Xia W, Qiu B, Xia D, Zou R (2013). Facile preparation of hierarchically porous carbons from metal-organic gels and their application in energy storage. *Scientific Reports*, 3(1): 1935
- Xiang R, Liu J C, Xu Y, Liu Y Q, Nai C X, Dong L, Huang Q F (2020). Framework, method and case study for the calculation of end of life for HWL and parameter sensitivity analysis. *Scientific Reports*, 10(1): 19509
- Xu Z X, Deng X Q, Zhang S, Shen Y F, Shan Y Q, Zhang Z M, Luque R, Duan P G, Hu X (2020). Benign-by-design N-doped carbonaceous materials obtained from the hydrothermal carbonization of sewage sludge for supercapacitor applications. *Green Chemistry*, 22(12): 3885–3895
- Yakaboylu G A, Jiang C, Yumak T, Zondlo J W, Wang J, Sabolsky E M (2021). Engineered hierarchical porous carbons for supercapacitor

- applications through chemical pretreatment and activation of biomass precursors. *Renewable Energy*, 163: 276–287
- Yue X M, An Z Y, Ye M, Liu Z J, Xiao C C, Huang Y, Han Y J, Zhang S Q, Zhu J S (2019). Preparation of porous activated carbons for high performance supercapacitors from Taixi anthracite by multi-stage activation. *Molecules (Basel, Switzerland)*, 24(19): 3588
- Yui K, Kuramochi H, Osako M (2018). Understanding the behavior of radioactive cesium during the incineration of contaminated municipal solid waste and sewage sludge by thermodynamic equilibrium calculation. *ACS Omega*, 3(11): 15086–15099
- Zhang J, Deng R J, Ren B Z, Hou B, Hursthouse A (2019). Preparation of a novel $\text{Fe}_3\text{O}_4/\text{HCO}$ composite adsorbent and the mechanism for the removal of antimony (III) from aqueous solution. *Scientific Reports*, 9(1): 13021